HHS Public Access

Author manuscript

J Orthop Res. Author manuscript; available in PMC 2021 November 01.

Published in final edited form as:

J Orthop Res. 2020 November ; 38(11): 2484–2494. doi:10.1002/jor.24648.

Platelet Derived Growth Factor Receptor-β (PDGFRβ) lineage tracing highlights perivascular cell to myofibroblast transdifferentiation during post-traumatic osteoarthritis.

Takashi Sono, MD, PhD[1,2], **Ching-Yun Hsu, BDS, MS**[1], **Stefano Negri, MD**[1], **Sarah Miller, BS**[1], **Yiyun Wang, PhD**[1], **Jiajia Xu, PhD**[1], **Carolyn A Meyers, BS**[1], **Bruno Peault, PhD**[3,4], **Aaron W. James, MD, PhD**[1,3]

[1]Department of Pathology, Johns Hopkins University, Ross Research Building, Room 524A, 720 Rutland Avenue, Baltimore, MD, 21205, United States.

[2]Department of Orthopedic Surgery, Graduate School of Medicine, Kyoto University, 54 Shogoin Kawahara-cho, Sakyo-ku, Kyoto 606–8507, Japan.

[3]UCLA and Orthopaedic Hospital Department of Orthopaedic Surgery and the Orthopaedic Hospital Research Center, 90095, University of Edinburgh, Edinburgh, United Kingdom

[4]Center For Cardiovascular Science and MRC Center for Regenerative Medicine, University of Edinburgh, Edinburgh, United Kingdom

Abstract

Pericytes ubiquitously surround capillaries and microvessels within vascularized tissues, and have diverse functions after tissue injury. In addition to regulation of angiogenesis and tissue regeneration after injury, pericytes also contribute to organ fibrosis. Destabilization of the medial meniscus (DMM) phenocopies post-traumatic osteoarthritis, yet little is known regarding the impact of DMM surgery on knee-joint associated pericytes and their cellular descendants. Here, inducible PDGFRβ-CreER^{T2} reporter mice were subjected to DMM surgery, and lineage tracing studies performed over an 8 week period. Results showed that at baseline PDGFRβ reporter activity highlights abluminal perivascular cells within synovial and infrapatellar fat pad (IFP) tissues. DMM induces a temporospatially patterned increase in vascular density within synovial and subsynovial tissues. Marked vasculogenesis within the infrapatellar fat pad (IFP) was accompanied by expansion of PDGFRβ reporter^{+} perivascular cell numbers, detachment of mGFP^{+} descendants from vessel walls, and aberrant adoption of myofibroblastic markers among mGFP^{+} cells including aSMA, ED-A, and TGF-β1. At later timepoints, fibrotic changes and vascular maturation occurred within subsynovial tissues, with redistribution of PDGFRβ^{+} cellular descendants back to their perivascular niche. In sum, PDGFRβ lineage tracing allows for tracing of perivascular cell fate within the diarthrodial joint. Further, destabilization of the joint induces

Corresponding author: Aaron W. James, MD, PhD, Department of Pathology, Johns Hopkins University, Ross Research Building, Room 524A, 720 Rutland Avenue, Baltimore, MD, 21205, United States. awjames@jhmi.edu Tel: +1(410) 502-4143.

Author contribution statement

The conception and design (TS and AWJ) of the study, acquisition of data (TS, CH and SN), material collection (TS, CH, YW, JX and CAM), analysis and interpretation of data (TS, SN, BP and AWJ), drafting the article (TS, SM and AWJ) or revising it critically for important intellectual content (TS, BP and AWJ) and final approval of the version to be submitted (all authors).

vascular and fibrogenic changes of the IFP accompanied by perivascular to myofibroblast transdifferentiation.

Keywords

Pericyte; PDGFRβ; perivascular stem cell; myofibroblast; DMM

Introduction

Pericytes ubiquitously surround capillaries and microvessels within vascularized tissues, and have diverse functions after tissue injury. In addition to regulation of angiogenesis after injury[1], pericytes have demonstrated tissue-intrinsic regenerative properties[2,3] and immunomodulatory features[4,5], but also contribute to organ fibrosis[6]. For example within the kidney, lineage tracing demonstrates that pericytes derived from Fox D1 positive mesenchymal cells[7] or Gli1 positive cells[6] contribute to renal fibrosis after injury. Within the lung, an analogous population of pericytes represents an important pool of myofibroblast progenitors responsible for interstitial fibrosis[8,9]. Within the rotator cuff, PDGFRα and PDGFRβ expressing pericytes contribute to fibro-adipogenic degeneration after injury[10]. Thus, and in a context dependent manner, pericytes (or subsets of mural cells within the microvasculature) demonstrate pro-fibrotic features after tissue injury.

The morphologic features that accompany cartilage degradation changes after trauma are numerous. These are best understood within the destabilization of the medial meniscus (DMM) model[11], but are broadly applicable to degenerative changes in human OA[12]. Within the synovium and subsynovium, vascular proliferation, mild acute and chronic synovitis, hyperplasia of synoviocytes[13] and leukocyte infiltration between adipocytes have been described[14]. These changes are followed by accumulation of collagenous extracellular matrix and fibrosis of the infrapatellar fat pad (IFP)[14]. However, the role of pericytes and other perivascular cells within the contexts of these robust morphologic changes of the synovium have not been defined.

Here, we utilized transgenic PDGFRβ-CreER^{T2};mT/mG reporter mice to document the cellular kinetics and cell fate of pericytes within the knee joint after DMM surgery. Our findings demonstrate a temporospatially defined expansion of perivascular cellular descendants after DMM within the stifle joint. PDGFRβ^{+} descendants detached from vessels walls within the subsynovial tissues and adopted myofibroblast markers, consistent with perivascular to myofibroblast transdifferentiation.

Methods

Animals

All animal studies were performed with institutional ACUC approval within Johns Hopkins University, complying with all relevant ethical regulations (ACUC protocol # MO18M12). PDGFRβ-CreER^{T2} and mT/mG mice were purchased from Jackson lab (stock No.029684 and No.007676). PDGFRβ-CreER^{T2} and mT/mG mice were crossed to generate PDGFRβ-CreER^{T2}; mT/mG mice. Both genders of these animals were used. Animals were bred and

housed under SPF conditions with no more than four adult mice per cage. 200μg of tamoxifen (TM, Sigma, T5648) dissolved in corn oil was injected intraperitoneally to PDGFRβ-CreER^{T2}; mT/mG mice at the age of 8 weeks for 4 days consecutively, using a previously validated TM administration schedule[15]. Essentially no recombination was observed within the joint associated tissues with injection of TM free vehicle control.

Destabilization of the medial meniscus

Destabilization of the medial meniscus (DMM) or sham surgery were performed at the age of 10 weeks, in similarity to prior reports[16]. Animals were randomly allocated to treatment groups. Briefly, left hindlimbs were disinfected with povidone-iodine and 70% ethanol, and Buprenorphine SR (1mg/kg) was injected subcutaneously. A 1 cm longitudinal incision was made on the medial aspect of the knee joint under general anesthesia using 2% isoflurane, and blunt dissection of the joint capsule along the medial side of the patellar ligament was performed to expose the medial menisco-tibial ligament (MMTL). The MMTL was transected using a 11-blade scalpel to destabilize the medial meniscus. The medial joint capsule and the skin were closed with 5–0 prolene. The sham surgery was performed with a similar surgical approach without transection of the joint capsule and the MMTL.

Micro computed tomography imaging

Knee joints were dissected and scanned with a SkyScan1175 (Bruker, MA, USA) high-resolution micro CT imaging system at 65 kV and 153 μA with a 1.0-mm aluminum filter to obtain a 10 μm voxel size. The images were reconstructed using CT Vox Micro-CT Volume Rendering Software (Bruker).

Histology and histomorphometry

Uninjured mice were sacrificed at the age of 10 weeks. In DMM or sham surgery groups, animals were sacrificed at either 2 weeks or 8 weeks postoperatively. Specimens were fixed in 4% paraformaldehyde for 24 hours, decalcified with 14% ethylenediaminetetraacetic acid (EDTA) for 14 days, and embedded in the optimum cutting temperature (OCT) compound. Sections were prepared at 6 μm thickness with a Cryofilm type 3c (SECTION-LAB, Japan).

For immunofluorescent immunohistochemistry, sections were washed in 1× PBS, blocked in 5% normal goat serum (S-1000, Vector Labs, CA, USA) for 30 min, and incubated with primary antibodies specific for CD31 (1:50, ab28364, Abcam, MA, USA), α-SMA (1:400, ab7817, Abcam), ED-A fibronectin (1:400, F6140, Sigma Aldrich, MO, USA) or TGF-β1(1:400, ab92486, Abcam) at 4 °C overnight. Sections were then incubated with Alexa Fluor® 647-conjugated secondary antibodies (1:200, ab150083 or ab150119, Abcam), and mounted with mounting medium containing DAPI (H-1500, Vector Labs). Bright field images were obtained on a Leica DM 6B microscope (Leica Biosystems, Germany). Immunofluorescent images were acquired on a LSM 780 FCS confocal microscope (Carl Zeiss, Germany).

OARSI scoring of the knee joints

Three frozen semi-serial sagittal sections with 36 μm intervals were prepared from the medial compartment of each mouse knee joint to represent the weight-bearing area of the

distal femur and proximal tibia. Sections were stained with safranin O and fast green. Cartilage injury was scored using the OARSI scoring system, based on prior reports[17]. The average scores of both femur and tibia were summed. All scoring was performed blinded to treatment group.

Synovial scoring of the knee joints

Frozen sagittal sections at the level of the posterior cruciate ligament were stained with hematoxylin and eosin. Synovitis was scored using previously published synovitis scoring criteria[18], ranging from 0 (minimal inflammation) to 6 (maximal synovitis). All scoring was performed blinded to treatment group.

Fibrosis scoring of the knee joint.

Frozen sagittal sections at the level of the posterior cruciate ligament were stained with Masson's trichrome stain. Semiquantitative evaluation was performed according to the method previously described[19]. In short, score 0 indicates normal (fibrosis is less than 20% of total area), score 1: low (20–40%), score 2: high (40–60%), score 3: extensive (more than 60%). All scoring was performed blinded to treatment group.

Morphometric analyses

All morphometric analyses of the knee joints were performed under 10x field (a single representative image was obtained per slide per animal) using Photoshop (Adobe) or Zen software (Carl Zeiss). Vascular number was defined by CD31-positive vessels. PDGFRβ density and vascular area were measured by the sum of PDGFRβ positive and CD31 positive areas divided by total measured area of the specified tissues (cartilage, adipose area, perivascular area, synovium and ligament) and presented as percentages. Vascular diameters were calculated by averaging the maximum diameter of the individual vessels. Non-vascular PDGFRβ density was calculated by the subtraction of PDGFRβ positive vascular area from PDGFRβ total density. PDGFRβ coverage was calculated as the percentages of the PDGFRβ positive vessels out of total vessel numbers. We focused on the anterior to middle portions of the knee joint. There were five areas of interest in the knee joint: articular cartilage, adipose areas of IFP, perivascular areas of IFP, synovium and ligament. Cartilage surfaces of the knee joints that are highlighted as tdTomato positive in immunofluorescent images are defined as cartilage areas. The upper region of the IFP was defined as adipose area[19]. The lower region of the IFP was defined as the perivascular area[19]. All quantifications were based on random 10x field images. All morphometric analyses were performed blinded to treatment group.

Flow cytometry analysis

As above, PDGFRβ-CreER^{T2}; mT/mG mice were injected Tamoxifen 2 week in advance and underwent sham or DMM surgery. Two weeks later, 11 IFPs in each group were collected by microdissection, pooled, minced and digested with Collagenase Type 2 (Worthington, NJ, USA), 0.5% BSA and MEMα(Gibco, NY, USA) for 1.5 hours at 37°C. Cells were analyzed with LSR II (BD Biosciences, USA) using FACS Diva software (BD

Biosciences) and Flow Jo v10 software (Tree Star, Inc, OR, USA). Cell debris was excluded based on size characterization.

Statistical analysis

Wilcoxon rank sum tests were performed to analyze all data. Sham groups were selected as controls. All statistical analyses were performed using GraphPad Prism8 (GraphPad Software, USA) and JMP13 (SAS Institute Inc, USA). P values <0.05 were considered statistically significant.

Results

Confirmation of osteoarthritic changes after DMM surgery

First, we confirmed that PDGFRβ reporter animals underwent degenerative changes after destabilization of the medial meniscus (DMM) surgery (Fig. 1). For these experiments, tamoxifen (TM) was administered to PDGFRβ-CreER^{T2}; mT/mG transgenic mice for 4 consecutive days at 8 weeks of age (Fig. 1A). Animals were subjected to DMM or sham surgery at 10 weeks of age (n=3 in each group), and analyzed 2 and 8 weeks thereafter. An uninjured group (n=3) was also made to examine the baseline joint state at 10 weeks of age. Micro computed tomography (μCT) of the left stifle joint confirmed destabilization of the medial meniscus among the DMM treatment groups at 2 and 8 weeks post-operative (Fig. 1B, white arrowheads). Sagittal histologic sections of the joint were next stained with Safranin O / Fast Green (Fig. 1C, D). Results confirmed a significant and progressive degeneration of the anterior horn of medial meniscus (Fig. 1C, black arrowhead) and loss of Safranin O staining among DMM (Fig. 1D, black asterisk) but not sham operated or uninjured animals (Fig. 1C, white arrowhead, Fig. 1D, white asterisk). These findings were most notable within the proximal tibial articular cartilage (T), but also evident within the distal femoral cartilage (F). Confirmation of degenerative changes was further obtained using the OARSI scoring system (Fig. 1E).

Synovitis and subsynovial fibrosis after DMM surgery

Having confirmed osteoarthritic changes after DMM, we next examined in detail the histologic changes within the infrapatellar fat pad (IFP) after either sham or DMM surgery. For this purpose, sagittal sections of the knee joint were obtained at the level of the posterior cruciate ligament (Fig. 2). Results using routine H&E stained sections showed dynamic changes in the appearance of the IFP (Fig. 2A, B). At two weeks after DMM, an inflammatory infiltrate was noted in the IFP, composed primarily of mononuclear inflammatory cells. At 8 weeks after DMM, the area of fibrosis of the IFP decreased. Inflammatory changes within the IFP and overlying synovium were next quantified using a semi-quantitative scoring system (Fig. 2C). Synovitis score was highest at 2 weeks post DMM and remained elevated above baseline at 8 weeks post DMM (Fig. 2C). In comparison and as expected, no significant synovitis was observed among uninjured or sham operated animals. Fibrotic change within the IFP was next confirmed by Masson’s trichrome staining (Fig. 2D). Here fibrotic change was most notable, as blue stained collagen fibers, within the IFP at 2 weeks post DMM, while fibrotic changes were still appreciable at 8 weeks post

DMM. In contrast, IFP fibrosis was not observed under uninjured or sham operated conditions. A semi-quantitative fibrosis score supported these results (Fig. 2E).

PDGFRβ lineage tracing images after DMM surgery

Having confirmed temporally patterned changes within the IFP elicited by DMM surgery, we next set out to examine pericyte reporter activity within the IFP using PDGFRβ reporter animals (Fig. 3A). For this purpose, the IFP was separated for analysis into adipose and perivascular areas (19) (Fig. 3B, C). Immunohistochemical staining for CD31 was performed to mark endothelium (Fig. 3B, C, appearing white), while PDGFRβ reporter activity appears green. Under uninjured conditions within the IFP, PDGFRβ reporter activity was found essentially exclusively within an abluminal 'pericytic' location. These findings were essentially confirmed among the IFP of sham-operated animals at both 2 and 8 weeks post-operative. In contrast, vascular changes and perivascular reporter activity showed dynamic changes after DMM surgery. At two weeks post-operative, numerous thin-caliber, capillary type vessels were observed within the IFP, either within adipose or perivascular locations (Fig. 3B, C, white arrowheads). This apparent increase in microvascular density was accompanied by a robust increase in the number of PDGFRβ reporter positive cells. Interestingly, DMM induced a significant expansion of PDGFRβ positive cellular descendants which was most notable at 2 weeks post-destabilization. Interestingly, cellular descendants of PDGFRβ reporter positive cells were frequent both in a pericytic location, but also in cells completely unassociated with microvessels. Similar observations were made at 8 weeks after DMM (Fig. 3B, C, far right column). Here, microvessels were still more apparent in comparison to uninjured or sham-operated conditions. PDGFRβ reporter activity was likewise increased over baseline. Again, both vascular-associated and non-vascular GFP reporter activity were observed.

Quantification of PDGFRβ lineage tracing images after DMM surgery

These qualitative changes in vascular patterning as well as cellular descendants of PDGFRβ-expressing perivascular cells induced by DMM were next quantified by histomorphometric analysis. First, vascular histomorphometry was performed on serial sections of IFPs under each treatment condition (Fig. 4A–C). Vascular histomorphometry was performed specifically within adipose areas, perivascular areas, or total IFP area (15). A significant increase in vascular numbers per 10x field was observed at both 2 and 8 weeks post DMM in comparison to sham-operated conditions (Fig. 4A). Statistically significant changes in mean vascular diameter were found at 8 weeks (Fig. 4B). Total vascular area showed a significant increase at both 2 and 8 weeks post DMM in comparison to sham-operated conditions (Fig. 4C). PDGFRβ pericyte reporter activity was next quantitatively examined within the IFP under each treatment condition and timepoint (Fig. 4D–F). Consistent with our prior observation, the density of PDGFRβ reporter activity was most notably increased at 2 weeks post DMM (Fig. 4D). A significant change in PDGFRβ reporter activity was also seen in adipose areas at 8 weeks post-DMM (Fig. 4D). The density of PDGFRβ reporter activity that was not associated with the vasculature was next quantified (Fig. 4E). Consistent with our prior observations, uninjured animals essentially showed minimal non-vascular PDGFRβ reporter activity within the IFP. These findings of rare to absent non-vascular reporter activity were likewise observed under sham-operated conditions. In contrast,

significantly increased numbers of non-vascular PDGFRβ reporter activity was observed at 2 weeks post-DMM (Fig. 4E). This remained elevated above baseline at 8 weeks post-DMM (Fig. 4E). Finally, the frequency of PDGFRβ positive pericytic coverage of microvessels within the IFP was assessed (Fig. 4F). Under uninjured conditions, essential 100% coverage of microvessels by PDGFRβ positive pericytes was observed. These findings of near universal PDGFRβ positive coverage were conserved among sham-operated animals. In contrast, PDGFRβ positive coverage was reduced after DMM. This finding was most notable at 2 weeks after injury (Fig. 4F) but found at 8 weeks post-DMM as well. In summary, destabilization surgery results in dynamic temporal changes in vascularization of the IFP, which was accompanied by expansion of PDGFRβ$^+$ cellular descendants, their detachment and subsequent reincorporation into vessel walls.

Flow cytometry quantification of PDGFRβ lineage tracing after DMM surgery

Flow cytometry was next performed as further confirmation of DMM induced expansion of PDGFRβ-expressing cellular descendants (Figure 5). The IFP with synovial lining was microdissected 2 weeks after sham or DMM surgery, and pooled for flow cytometric analysis of mGFP reporter activity (11 pooled synovial-IFP samples per condition). Total cell yields were significantly greater after DMM, accounting for an approximate 9.2 fold increase in cell frequency per synovial-IFP samples (113 cells per synovial-IFP samples under sham-operated conditions versus 1,045 cells per synovial-IFP samples after DMM). Both the absolute numbers and percentages of mGFP positive cells were increased post DMM. Specifically, mGFP+ cells increased from 3 events under sham-operated conditions (0.242% of total) to 401 events under DMM operated conditions (3.49% of total) (Fig. 5A,B).

PDGFRβ-expressing cellular descendants demonstrate myofibroblast markers after DMM surgery.

Our findings thus far suggested that DMM induces PDGFRβ positive pericyte expansion and detachment within the IFP, which was followed by fibrotic change of the IFP. These findings suggested the transdifferentiation of PDGFRβ-expressing pericytes to myofibroblasts within the IFP. To begin to investigate this possibility, immunohistochemistry for α-smooth muscle actin (α-SMA) was performed on the IFP of uninjured, sham-operated or DMM-operated animals (Fig. 6 and Supplementary Fig. 1). Results among uninjured and sham-operated animals showed that α-SMA immunostaining highlights only a thin rim of tissue within a pericytic / perivascular location (observed at both 2 and 8 weeks after sham surgery) (Fig. 6A,B). In marked contrast, a high density of α-SMA immunoreactivity was observed at 2 weeks post-DMM, which showed partial overlap with non-vascular mGFP/ PDGFRβ reporter activity (Fig. 6C and D, 39.7% of mGFP$^+$ cells showed α-SMA immunoreactivity). At 8 weeks post DMM, some residual α-SMA immunohistochemical staining was observed within non-vascular components of the IFP (Supplementary Fig. A). Thus, transient and robust α-SMA expression is observed within the IFP, including within mGFP+ pericyte descendants.

We used additional putative myofibroblast markers or related proteins such as ED-A fibronectin[20] (Fig. 6E–H, Supplementary Fig.1B) and TGFβ−1[20] (Fig. 6I–L, Supplementary

Fig. 1C). A similar expression pattern for both antigens was found. 88.6% and 74.3% of mGFP$^+$ cells showed ED-A staining and TGFβ−1 staining at 2 weeks after DMM, respectively. These findings suggested a marked enrichment in myofibroblast markers within the IFP, including within perivascular descendants, suggestive of myofibroblast transdifferentiation elicited by destabilization surgery.

PDGFRβ reporter activity in synovium, ligament and articular cartilage.

Finally, the specificity of PDGFRβ reporter activity within other joint-associated tissues was assessed. As mentioned, PDGFRβ reporter activity within the IFP was highly sensitive for perivascular cells. Our findings, however, also showed that PDGFRβ reporter activity was present in other cell types within joint-associated tissues. First, a small population of synoviocytes demonstrated PDGFRβ reporter activity (Fig. 7A,B). Interestingly, a slight and non-significant increase in numbers of PDGFRβ$^+$ synoviocytes was observed after DMM surgery, especially at the 8 week timepoint. Second, PDGFRβ-labeled cells were also found in the ligaments and tendons (Fig. 7C,D, see also Fig. 3A). No significant changes in PDGFRβ frequency within ligamentous cells was observed across treatment groups or timepoints. Third, a very rare population of PDGFRβ positive cells was identified within chondrocytes of articular cartilage (Fig. 7E, green), which were unchanged in frequency after DMM (Fig. 7F). In summary, while PDGFRβ reliably highlights pericytes, other joint-associated cell types also demonstrate reporter activity to a lesser degree.

Discussion

Pericytes and other perivascular cells have diverse functions in contexts of tissue repair, including modulating vascularization and immune response, as well as directly participating in repair or fibrosis. Our results within the context of destabilization of the stifle joint suggest that PDGFRβ-expressing pericytes play a dynamic role in the histologic changes of joint-associated tissues. Lineage tracing suggests that destabilization induces a series of events including PDGFRβ-expressing expansion, microvascular proliferation, and pericyte detachment along with aberrant expression of myofibroblast markers. With time, fibrosis and vascular maturation occurs with a return of PDGFRβ-expressing cellular descendants to their perivascular niche. Although not yet addressed, it is possible that acute increases in PDGFRβ$^+$ perivascular cells after destabilization have paracrine effects on cartilage catabolism in this model.

Myofibroblasts were first observed in granulation tissue of healing cutaneous wounds, in which they play a role to produce contractile force for wound closure[21]. Myofibroblasts have actin microfilaments with associated contractile proteins such as non-muscle myosin and stress fibers, which transmit force to the surrounding extracellular matrix[22]. Signaling pathways that regulate myofibroblastic differentiation include TGFβ and PDGF signaling, among others[23,]. The cellular origin of myofibroblasts appears to be diverse and contextually dependent, including dermal fibroblasts in cutaneous injury[22], portal fibroblasts and hepatic stellae cells in hepatic scarring[22], and also pericytes / perivascular cells in renal fibrosis[7].

Our findings within the IFP elicited by joint destabilization are analogous to findings in the tissue repair processes. Upon injury, perivascular MSC progenitors may drive the critical

remodeling of the affected organ, reducing its function dramatically. Resident Gli1$^+$ perivascular cells give rise to myofibroblasts upon renal, pulmonary, hepatic, or cardiac injury, contributing to organ failure, which is rescuable upon ablation of these cells[6]. Gli1$^+$ progenitors also contribute to vessel calcification[24], and in the bone marrow can be targeted pharmacologically with the Gli1 inhibitor GANT61 to prevent fibrosis[25]. Similarly, αv integrins on perivascular and interstitial cells in the skeletal and cardiac muscle contribute to fibrosis via TGF-β signaling[26]. Furthermore, a subset of PDGFRβ$^+$ perivascular cells co-expressing PDGFRα are highly fibrotic and contributes to fatty degeneration following massive tears of the mouse rotator cuff[27].

Recent research has made clear the diversity of mesenchymal cell types within the perivascular niche, and the increasingly complex heterogeneity of pericytes as both phenotypically and functionally diverse. For example, a developmental hierarchy of pericytes and other perivascular cells has been established by single-cell transcriptome analysis within human fat tissue[28] and, correlatively, these cell types have been shown to play distinct roles in osteogenesis *in vivo*[29]. Capoccia et al. found that bone marrow MSC like cells with high aldehyde dehydrogenase activity sustain better improvement of the ischaemic hind limb, as compared to the whole stromal cell population[30]. Perivascular cells and derived MSCs with superior chondrogenic potential have been identified by marker expression[31] and proximity to the joint[32]. Uniquely, subsets of pericytes and interstitial cells mediating either regeneration or pathologic fibrosis in the acutely injured skeletal muscle have been detected on expression of different combinations of PDGFRα and PDGFRβ[26,27]. Tissue-specific properties of human pericytes have been observed by other research groups. For example, muscle-associated human pericytes were more myogenic *in vitro* and *in vivo*[33]. Therefore, it is expected that the combinatorial analysis of multiple markers will allow to identify defined subsets of pericytes and their progeny with divergent roles in tissue repair or fibrosis.

In summary, transgenic inducible PDGFRβ reporter animals represent an excellent means to track pericytic cells within joint-associated tissues during development of osteoarthritis. Here, perivascular cell expansion, vascular detachment, and perivascular cell to myofibroblast transdifferentiation can be observed. As with many reporter animals, however, cell types within other tissue compartments also demonstrate reporter activity, and care must be taken to appropriately interpret histologic findings.

Supplementary Material

Refer to Web version on PubMed Central for supplementary material.

Acknowledgments

A.W.J. was supported by the NIH/NIAMS (R01 AR070773, K08 AR068316), NIH/NIDCR (R21 DE027922), USAMRAA through the Peer Reviewed Medical Research Program (W81XWH-180109121, W81XWH-18-1-0336), and Department of Defense through the Broad Agency Announcement (W81XWH-18-10613), American Cancer Society (Research Scholar Grant, RSG-18-027-01-CSM), the Maryland Stem Cell Research Foundation, and MTF Biologics. The content is solely the responsibility of the authors and does not necessarily represent the official views of the National Institute of Health, Department of Defense, or U.S. Army. AWJ is a member of the scientific advisory board for Novadip Biosciences for work unrelated to the current project.

References

1. Lindblom P, Gerhardt H, Liebner S, et al. 2003 Endothelial PDGF-B retention is required for proper investment of pericytes in the microvessel wall. Genes Dev 17: 1835–40. [PubMed: 12897053]
2. Volz KS, Jacobs AH, Chen HI, et al. 2015 Pericytes are progenitors for coronary artery smooth muscle. Elife 4: e10036. [PubMed: 26479710]
3. Crisan M, Yap S, Casteilla L, et al. 2008 A perivascular origin for mesenchymal stem cells in multiple human organs. Cell Stem Cell 3: 301–13. [PubMed: 18786417]
4. Chen CW, Okada M, Proto JD, et al. 2013 Human pericytes for ischemic heart repair. Stem Cells 31(2): 305–16. [PubMed: 23165704]
5. Meyers CA, Xu J, Zhang L, et al. 2017 Early immunomodulatory effects of implanted human perivascular stromal cells during bone formation. Tissue Eng Part A 24: 448–457. [PubMed: 28683667]
6. Kramann R, Schneider RK, DiRocco DP, et al. 2015 Perivascular Gli1+ progenitors are key contributors to injury-induced organ fibrosis. Cell Stem Cell 16(1): 51–66. [PubMed: 25465115]
7. Humphreys BD, Lin SL, Kobayashi A, et al. 2010 Fate tracing reveals the pericyte and not epithelial origin of myofibroblasts in kidney fibrosis. Am J Pathol 176: 85–97. [PubMed: 20008127]
8. Hung C, Linn G, Chow YH, et al. 2013 Role of lung pericytes and resident fibroblasts in the pathogenesis of pulmonary fibrosis. Am J Respir Crit Care Med 188(7): 820–30. [PubMed: 23924232]
9. Hung CF, Wilson CL, Schnapp LM. 2019 Pericytes in the Lung. Adv Exp Med Biol 1122: 41–58. [PubMed: 30937862]
10. Jensen AR, Kelley BV, Mosich GM, et al. 2018 Platelet-derived growth factor receptor α co-expression typifies a subset of platelet-derived growth factor receptor β-positive progenitor cells that contribute to fatty degeneration and fibrosis of the murine rotator cuff. J Shoulder Elbow Surg 27(7):1149–61. [PubMed: 29653843]
11. Glasson SS, Askew R, Sheppard B, et al. 2005 Deletion of active ADAMTS5 prevents cartilage degradation in a murine model of osteoarthritis. Nature 434: 644–8. [PubMed: 15800624]
12. Lorenz J, Grässel S. 2014 Experimental osteoarthritis models in mice. Methods Mol Biol 1194: 401–19. [PubMed: 25064117]
13. Bondeson J, Blom AB, Wainwright S, et al. 2010 The role of synovial macrophages and macrophage-produced mediators in driving inflammatory and destructive responses in osteoarthritis. Arthritis Rheum 62(3):647–57. [PubMed: 20187160]
14. Eymard F, Pigenet A, Citadelle D, et al. 2017, Knee and hip intra-articular adipose tissues (IAATs) compared with autologous subcutaneous adipose tissue: a specific phenotype for a central player in osteoarthritis. Ann Rheum Dis 76(6):1142–48. [PubMed: 28298375]
15. Park DY, Lee J, Kim J, et al. 2017 Plastic roles of pericytes in the blood-retinal barrier. Nat Commun 8:15296. [PubMed: 28508859]
16. Glasson SS, Blanchet TJ, Morris EA. 2007 The surgical destabilization of the medial meniscus (DMM) model of osteoarthritis in the 129/SvEv mouse. Osteoarthritis Cartilage 15: 1061–9. [PubMed: 17470400]
17. Pritzker KP, Gay S, Jimenez SA, et al. 2006 Osteoarthritis cartilage histopathology: grading and staging. Osteoarthritis Cartilage 14: 13–29. [PubMed: 16242352]
18. Lewis JS, Hembree WC, Furman BD, et al. 2011 Acute joint pathology and synovial inflammation is associated with increased intra-articular fracture severity in the mouse knee. Osteoarthritis Cartilage 19: 864–73. [PubMed: 21619936]
19. Inomata K, Tsuji K, Onuma H, et al. 2019 Time course analyses of structural changes in the infrapatellar fat pad and synovial membrane during inflammation-induced persistent pain development in rat knee joint. BMC Musculoskelet Disord 20: 8. [PubMed: 30611247]
20. Darby IA, Zakuan N, Billet F, Desmoulière. 2016 The myofibroblast, a key cell in normal and pathological tissue repair. Cell Mol Life Sci 73(6):1145–57. [PubMed: 26681260]
21. Gabbiani G, Ryan GB, Majne G. 1971 Presence of modified fibroblasts in granulation tissue and their possible role in wound contraction. Experientia 27: 549–50. [PubMed: 5132594]

22. Tomasek JJ, Gabbiani G, Hinz B, et al. 2002 Myofibroblasts and mechano- regulation of connective tissue remodelling. Nat Rev Mol Cell Biol 3: 349–63. [PubMed: 11988769]

23. Desmoulière A, Geinoz A, Gabbiani F, Gabbiani G. 1993 Transforming growth factor-beta 1 induces alpha-smooth muscle actin expression in granulation tissue myofibroblasts and in quiescent and growing cultured fibroblasts. J Cell Biol 122: 103–11. [PubMed: 8314838]

24. Kramann R, Goettsch C, Wongboonsin J, et al. 2016 Adventitial MSC-like Cells Are Progenitors of Vascular Smooth Muscle Cells and Drive Vascular Calcification in Chronic Kidney Disease. Cell Stem Cell 19(5):628–642. [PubMed: 27618218]

25. Schneider RK, Mullally A, Dugourd A, et al. 2017 Gli1+ Mesenchymal Stromal Cells Are a Key Driver of Bone Marrow Fibrosis and an Important Cellular Therapeutic Target. Cell Stem Cell 20(6):785–800. [PubMed: 28457748]

26. Murray IR, Gonzalez ZN, Baily J, et al. 2017 αv integrins on mesenchymal cells regulate skeletal and cardiac muscle fibrosis. Nat Commun 8(1):1118. [PubMed: 29061963]

27. Jensen AR, Kelley BV, Ariniello A, et al. 2018 Neer Award 2018: Platelet-derived growth factor receptor α co-expression typifies a subset of platelet-derived growth factor receptor β-positive progenitor cells that contribute to fatty degeneration and fibrosis of the murine rotator cuff. J Shoulder Elbow Surg 27(7):1149–1161. [PubMed: 29653843]

28. Hardy WR, Moldovan NI, Moldovan L, et al. 2017 Transcriptional Networks in Single Perivascular Cells Sorted from Human Adipose Tissue Reveal a Hierarchy of Mesenchymal Stem Cells. Stem Cells 35(5):1273–1289. [PubMed: 28233376]

29. Wang Y, Xu J, Chang L, et al. 2019 Relative contributions of adipose-resident CD146+ pericytes and CD34+ adventitial progenitor cells in bone tissue engineering. NPJ Regen Med 4:1 [PubMed: 30622740]

30. Capoccia BJ, Robson DL, Levac KD, et al. 2009 Revascularization of ischemic limbs after transplantation of human bone marrow cells with high aldehyde dehydrogenase activity. Blood 113(21):5340–51. [PubMed: 19324906]

31. Dickinson SC, Sutton CA, Brady K, et al. 2017 The Wnt5a Receptor, Receptor Tyrosine Kinase-Like Orphan Receptor 2, Is a Predictive Cell Surface Marker of Human Mesenchymal Stem Cells with an Enhanced Capacity for Chondrogenic Differentiation. Stem Cells 35(11):2280–2291. [PubMed: 28833807]

32. Hindle P, Khan N, Biant L, Péault B. 2016 The Infrapatellar Fat Pad as a Source of Perivascular Stem Cells with Increased Chondrogenic Potential for Regenerative Medicine. Stem Cells Transl Med 6(1):77–87. [PubMed: 28170170]

33. Dellavalle A, Sampaolesi M, Tonlorenzi R, et al. 2007 Pericytes of human skeletal muscle are myogenic precursors distinct from satellite cells. Nat Cell Biol 9(3):255–67. [PubMed: 17293855]

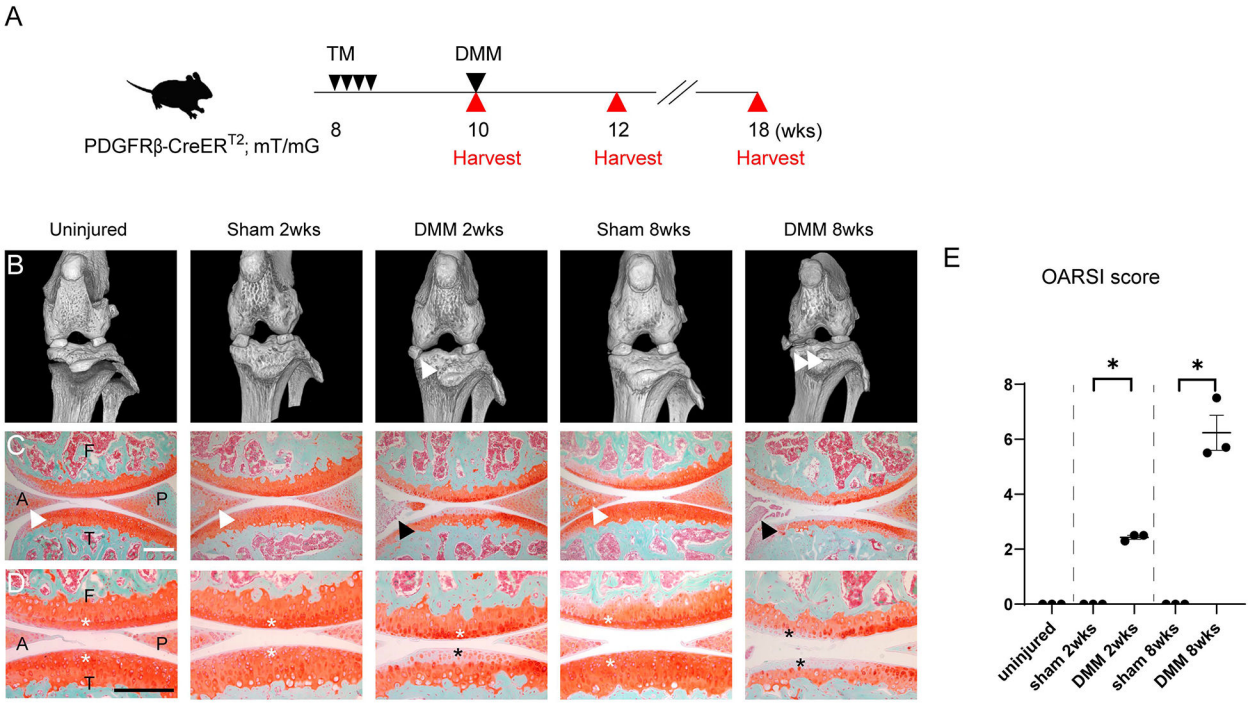

Figure 1.

Validation of DMM induced osteoarthritis within PDGFRβ-CreER^{T2} reporter animals. (A) Schematic of experiments, including tamoxifen (TM) injection daily to PDGFRβ-CreER^{T2}; mT/mG mice for 4 consecutive days at 8 weeks of age, followed by DMM surgery at 10 weeks of age. Analyses were performed at 2 and 8 weeks after DMM. (B) Micro computed tomography (microCT) images of the left knee joints of PDGFRβ-CreER^{T2}; mT/mG mice. White arrowheads indicate the displaced medial meniscus at 2 and 8 weeks post-operative among DMM treated groups. (C) Sagittal sections of the left knee joints of PDGFRβ-CreER^{T2}; mT/mG mice at the level of medial compartments. Safranin O- fast green staining. Anterior horns of the medial meniscus are indicated in the uninjured, sham 2 weeks and sham 8 weeks group with white arrowheads and in DMM 2 and 8 weeks with black arrowheads. (D) High magnifications of Safranin O- fast green staining. Cartilage surfaces were marked with white asterisks in control groups, with black asterisks in DMM groups. (E) OARSI scores. A: anterior horn of the medial meniscus, P: posterior horn of the medial meniscus, F: femur, T: tibia. Scale bars: 100μm. N=3 mice per group. *p<0.05.

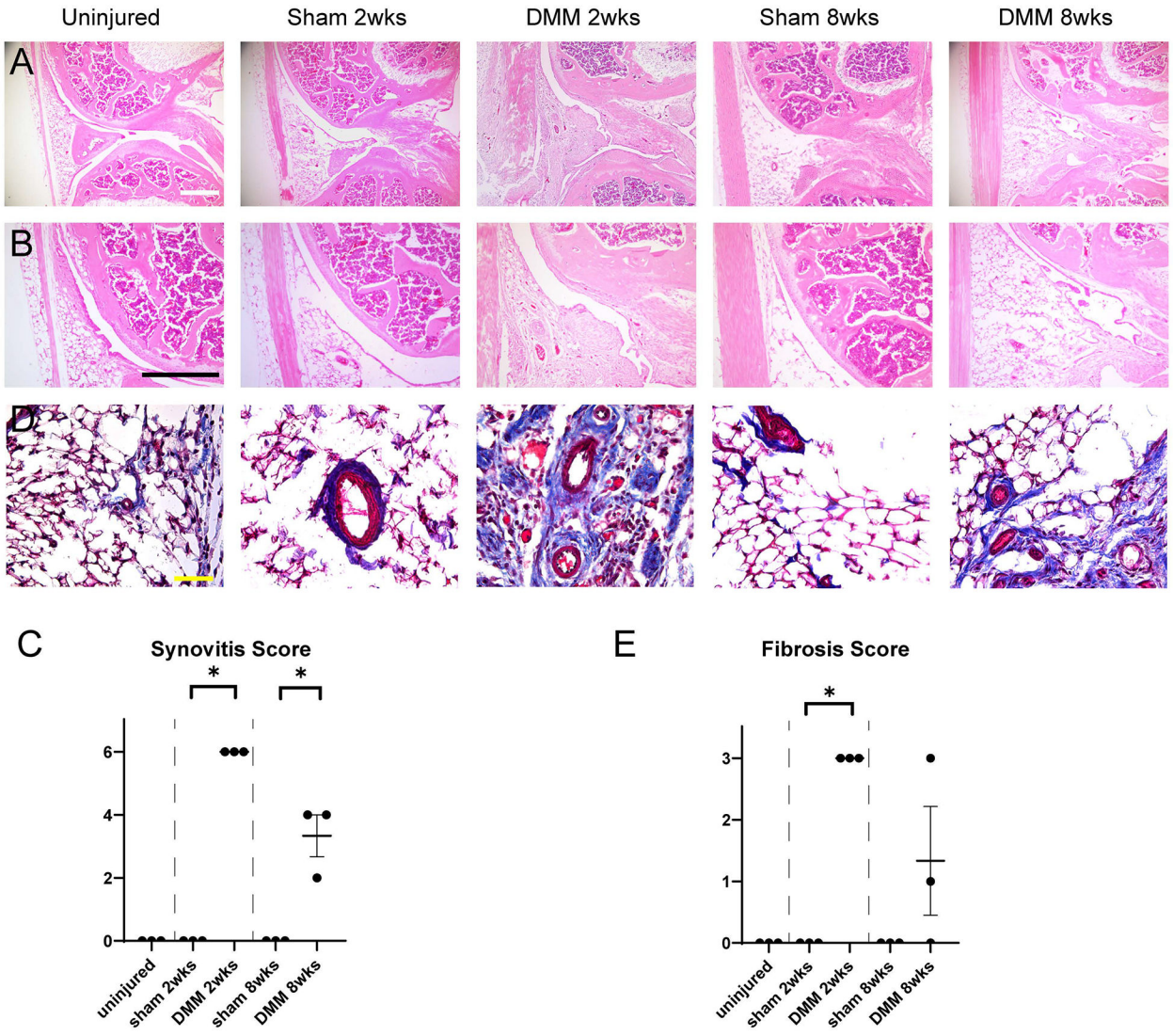

Figure 2.

Histologic changes within the IFP after DMM within PDGFRβ-CreER^{T2} reporter animals. (A,B) Sagittal sections of the left stifle joints of PDGFRβ-CreER^{T2}; mT/mG animals at the level of posterior cruciate ligaments. Hematoxylin and eosin (H&E) staining at low (A) and (B) high magnifications. Scale bars: 200 μm. (C) Synovitis scores within PDGFRβ-CreER^{T2}; mT/mG mice. (D) Masson Trichrome staining of the infrapatellar fat pad (IFP). Scale bars: 50 μm. (E) Fibrosis scores o within PDGFRβ-CreER^{T2}; mT/mG mice. N=3 mice per group. *p<0.05.

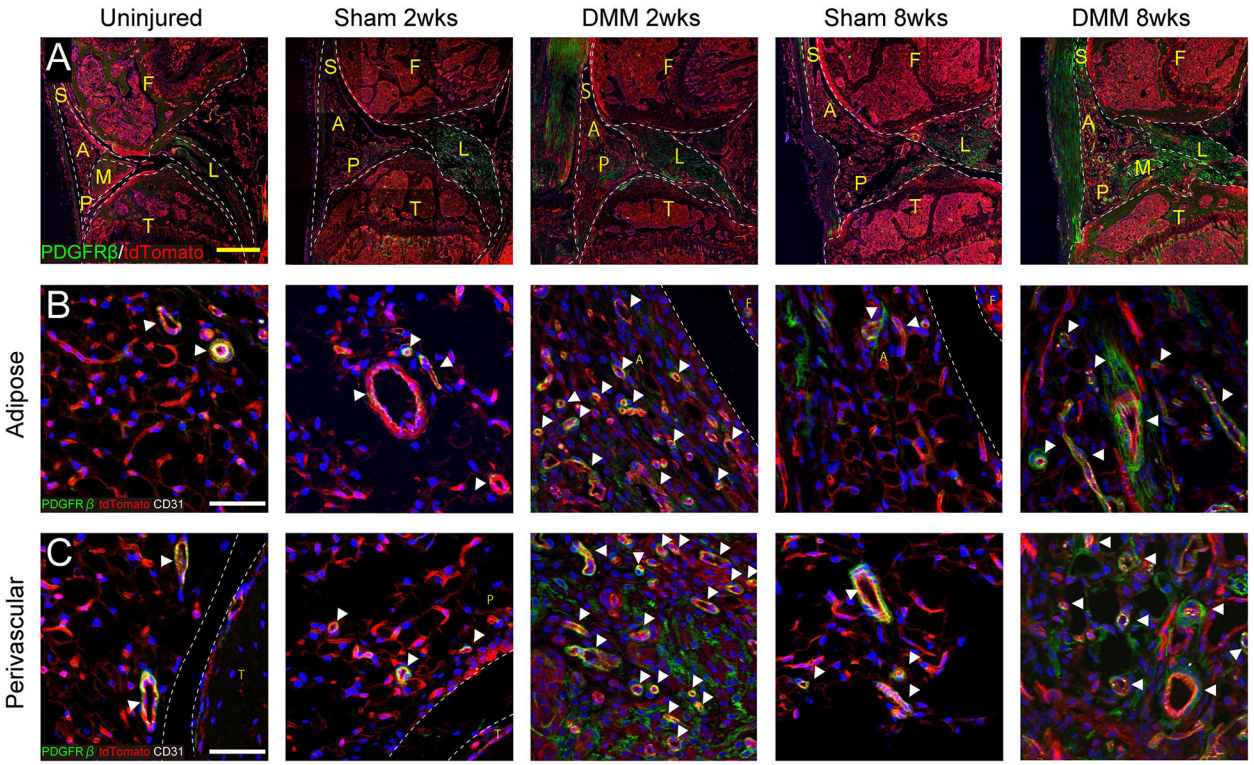

Figure 3.

PDGFRβ reporter activity with or without DMM. (A) Immunofluorescent images of the knee joints among PDGFRβ-CreER^{T2} reporter mice at the level of posterior cruciate ligaments. PDGFRβ reporter activity appears green, while all other cells appear red. DAPI nuclear counterstain appears blue. Scale bars: 200 μm. (B,C) High magnifications of PDGFRβ-CreER^{T2} reporter activity with CD31 immunofluorescent staining, within either (B) adipose or (C) perivascular areas. PDGFRβ reporter activity appears green, while CD31 immunostaining appears white. White arrowheads indicate vessels. Scale bars: 50 μm. S: Synovium, A: adipose area, P: perivascular area, F: femur, T: tibia, L: posterior cruciate ligament, M: meniscus. N=3 mice per group.

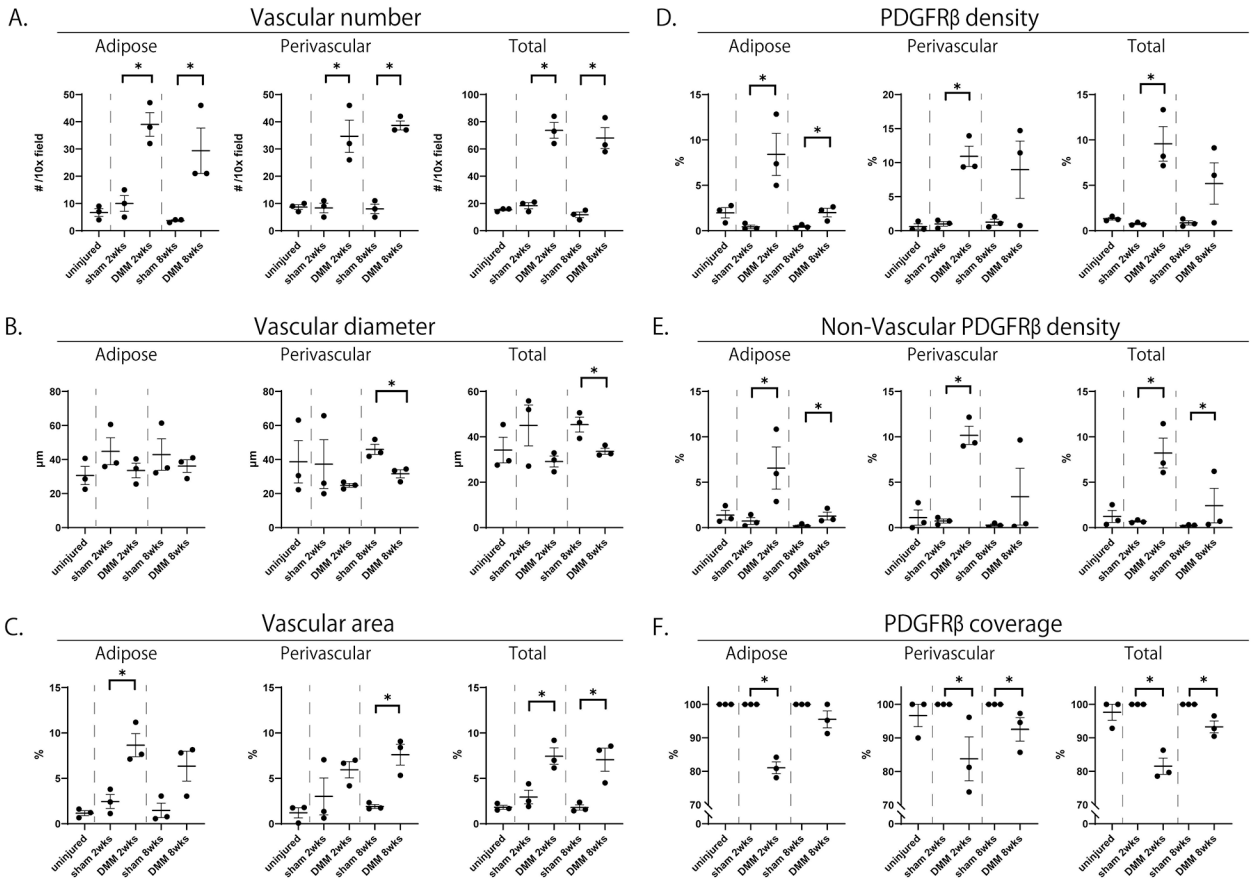

Figure 4.

Vascular histomorphometry and PDGFRβ reporter quantification with or without DMM. Corresponding images are shown in Figure 3. Quantifications performed specifically within (left) adipose, (middle) perivascular and (right) total areas of the IFP. (A) Blood vessel number per 10x field. (B) Mean blood vessel diameter. (C) Total blood vessel area. (D) Total PDGFRβ reporter activity. (E) Total non-vascular PDGFRβ reporter activity. (F) Vascular coverage with PDGFRβ reporter activity. N=3 mice per group. *p<0.05

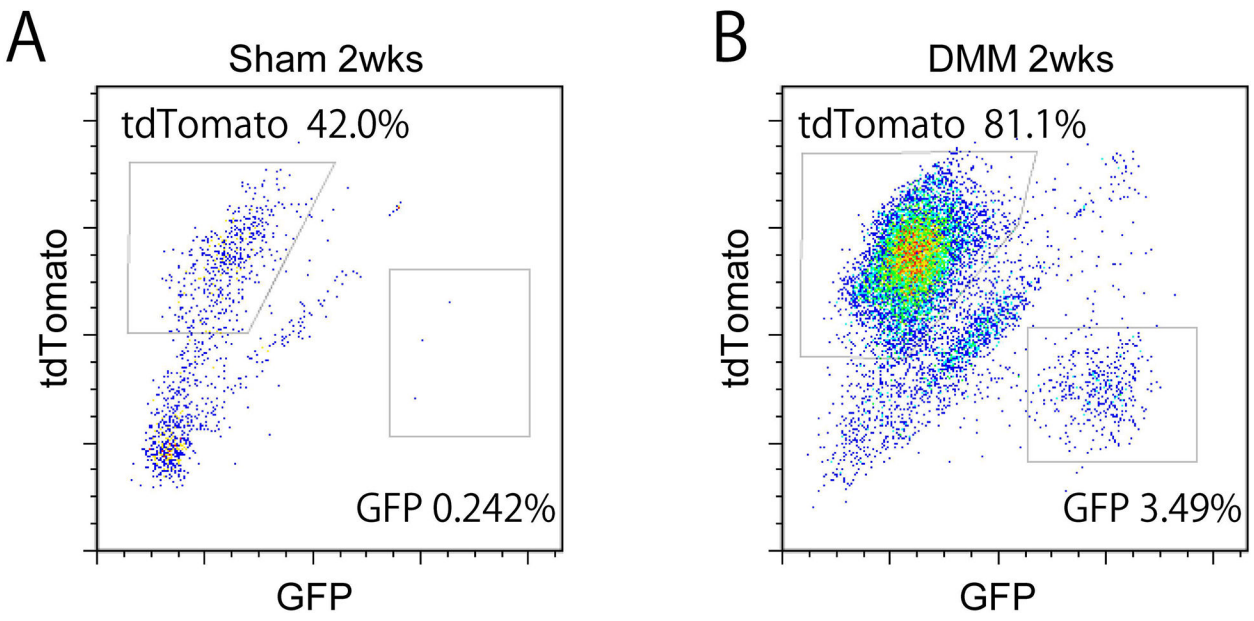

Figure 5.

Flow cytometry analysis and quantification of PDGFRβ reporter among microdissected IFP. Samples analyzed at 2 weeks post sham or DMM surgery among PDGFRβ reporter animals. Frequency of mGFP+ and TdTomato+ cells was assessed. (A) 2 weeks post sham surgery, and (B) post DMM surgery. N=11 pooled mice per group.

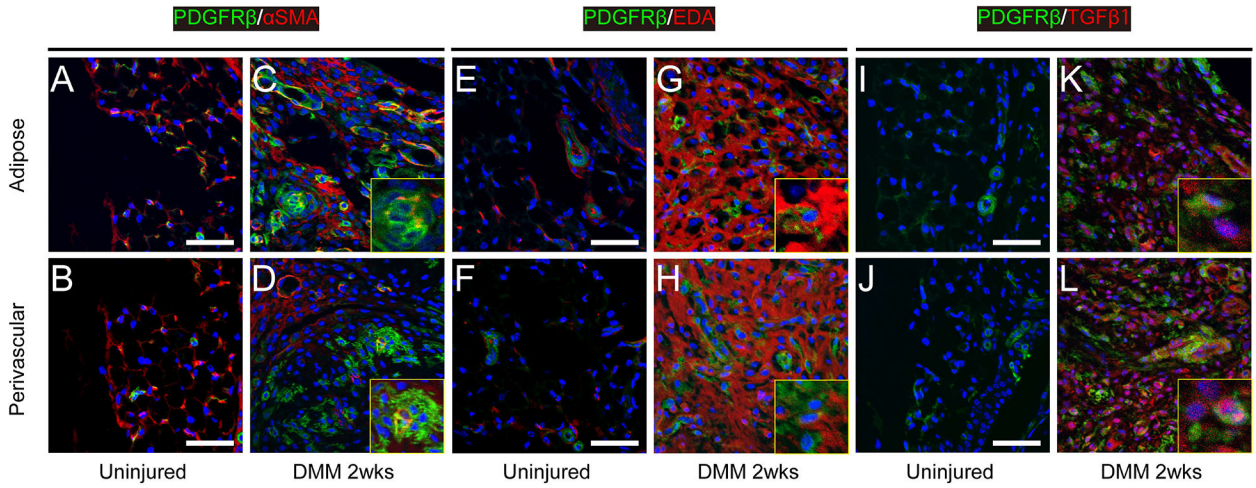

Figure 6.

Myofibroblast marker expression among uninjured and 2 weeks post DMM within PDGFRβ reporter animals. Images taken within representative adipose and perivascular areas of the IFP at the level of the posterior cruciate ligament. Across each image, PDGFRβ reporter activity appears green, while immunohistochemical staining appears red. DAPI nuclear counterstain appears blue. (A-D) α-SMA immunostaining, (E-H) ED-A fibronectin immunostaining, and (I-L) TGFβ−1 immunostaining. Small insets images are magnification of the region of interests. Additional corresponding images can be found in Supplementary Figure 1. Scale bars: 50 μm.

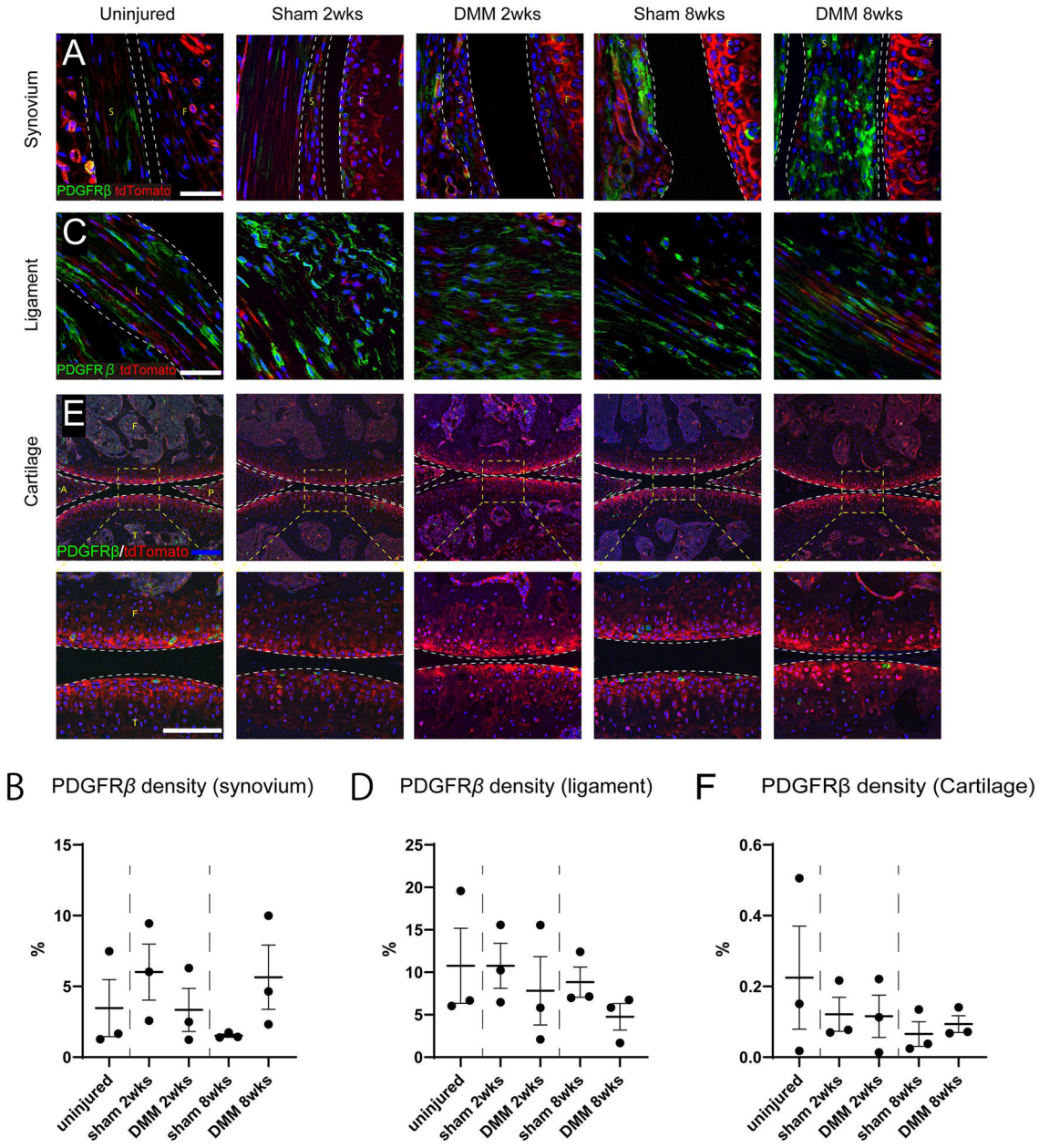

Figure 7.

Non-pericytic cellular sources of PDGFRβ reporter activity. (A) High magnification images of synovium of the knee joints at the level of posterior cruciate ligaments. Scale bar: 50 μm. (B) Quantification of PDGFRβ reporter activity within the synovium. (C) High magnification immunofluorescent images of posterior cruciate ligament of the stifle joint. Scale bars: 50 μm. (D) Quantification of PDGFRβ reporter activity within the posterior cruciate ligament. (E) Immunofluorescent images of the medial compartments of the knee joint so as to visualize any reporter activity within articular cartilage. Blue scale bar: 100 μm. High magnification images are in the lower row. White scale bar: 50μm. (F) Quantification of PDGFRβ reporter activity within articular cartilage. S: Synovium, F:

femur, T: tibia, L: posterior cruciate ligament. A: anterior horn of the medial meniscus, P: posterior horn of the medial meniscus. N=3 mice per group.